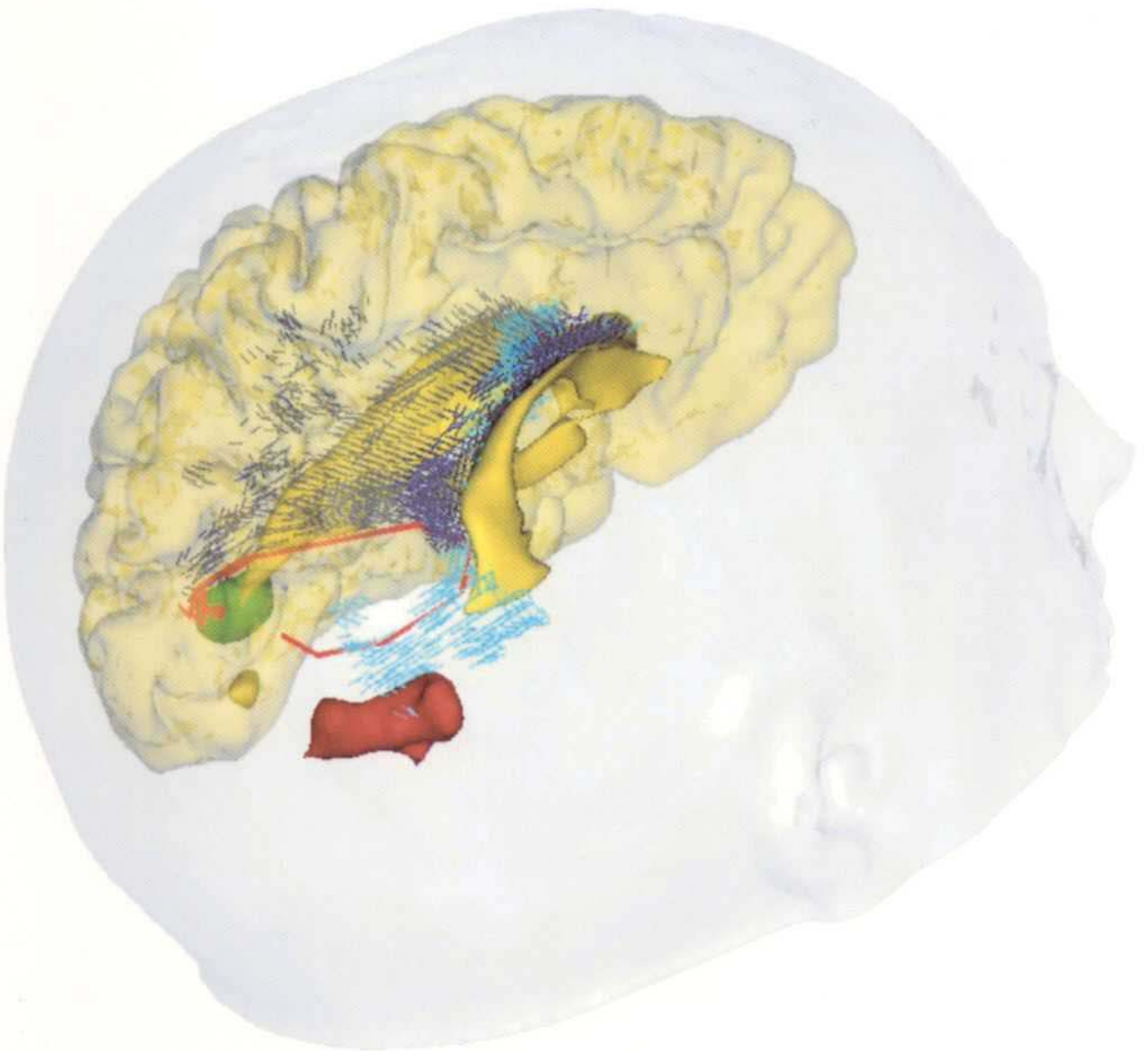


Journal of Cognitive Neuroscience

Volume 14, Number 4
May 15, 2002

Published by The MIT Press with the Cognitive Neuroscience Institute



Visualizing the Neural Bases of a Disconnection Syndrome with Diffusion Tensor Imaging

N. Molko¹, L. Cohen^{1,2}, J. F. Mangin³, F. Chochon²,
S. Lehericy², D. Le Bihan³, and S. Dehaene¹

Abstract

■ Disconnection syndromes are often conceptualized exclusively within cognitive box-and-arrow diagrams unrelated to brain anatomy. In a patient with alexia in his left visual field resulting from a posterior callosal lesion, we illustrate how diffusion tensor imaging can reveal the anatomical bases of a disconnection syndrome by tracking the degeneration of neural pathways and relating it to impaired fMRI activations and behavior. Compared to controls, an abnormal pattern of brain activity was observed in the patient during word reading, with a lack of activation of the left visual word form area (VWFA) by left-

hemifield words. Statistical analyses of diffusion images revealed a damaged fiber tract linking the left ventral occipito-temporal region to its right homolog across the lesioned area of corpus callosum and stopping close to the areas found active in fMRI. The behavioral disconnection syndrome could, thus, be related functionally to abnormal fMRI activations and anatomically to the absence of a connection between those activations. The present approach, based on the “negative tracking” of degenerated bundles, provides new perspectives on the understanding of human brain connections and disconnections. ■

INTRODUCTION

The cognitive impairments that can be observed in brain-lesioned patients are sometimes better explained by a disconnection between two cerebral processes than by primary damage to those processes themselves (Geschwind, 1965). However, disconnections are often conceptualized exclusively within cognitive box-and-arrow diagrams unrelated to brain anatomy. Up to now, the only way to identify the anatomical basis of interarea connections was the postmortem histological visualization of fiber pathways. Diffusion tensor imaging, a magnetic resonance technique, represents a new approach for the study of brain connectivity. This non-invasive technique allows the measurement of the Brownian motion of water molecules on a voxel-by-voxel basis, thus providing quantitative information on the microstructure of biological tissues. The motion of water molecules is modified by local tissue components such as cell membranes, organelles, and macromolecules. In particular, within cerebral white matter, the coherent orientation of axons constrains water molecules to move preferentially along the main direction of neural fibers. This introduces a measurable anisotropy in the diffusion, which can be quantified and gives information about the local density and coherence of axons in the

measured voxel. In particular, this anisotropy parameter has been shown to be highly sensitive to the degeneration of white matter tracts in brain-injured patients, in whom focal decreases in anisotropy can be observed (Werring et al., 2000). Furthermore, the direction of water diffusion itself can be measured with diffusion tensor MRI and can be used to infer the local orientation of fibers (Poupon et al., 2000; Conturo et al., 1999; Le Bihan, 1995).

In normal subjects, the local orientation vectors measured at each voxel location can then be connected together using computer algorithms to infer the long-range trajectory of entire fiber tracts (Poupon et al., 2000; Conturo et al., 1999). However, such tracking of neural pathways remains impeded by the insufficient spatial resolution, which results in tracing ambiguities due to the crossing of fiber bundles within the same voxel. Here, we describe a different approach, based on the “negative tracking” of degenerated bundles, which may circumvent some of these problems. The method consists in isolating a fiber tract by identifying, in a patient with a focal brain lesion, the set of voxels that present a statistically significant decrease in anisotropy and which presumably reflect the degeneration of an entire fiber tract. Like classical histological methods based on the tracking of degenerated axons after lesions, this method can be used to isolate a neural pathway within the otherwise complex and intermingled connections of the normal human brain. The trajectory of the degenerated pathway can then be compared with

¹INSERM, Service Hospitalier Frédéric Joliot, ²Hôpital de la Salpêtrière, ³UNAF, Service Hospitalier Frédéric Joliot, Commissariat à l’Energie Atomique

the outcome of computerized tracking algorithms in normal subjects.

Whether used in normals or patients, diffusion tensor imaging allows for the estimation of the anatomical trajectory of fiber tracts in a few minutes in a living subject using standard magnetic resonance equipment. Thus, diffusion MRI can easily be combined with functional magnetic resonance imaging, which gives access to information about the activation of brain areas in a given cognitive task. The two methods are complementary. Potentially, diffusion MRI can give access to the connectivity of the regions that are identified as coactivated during functional MRI. However, at present, this approach has not been used beyond the description of the projections from the lateral geniculate nucleus to occipital visual cortex (Conturo et al., 1999).

In the present article, we used this approach to study the connectivity underlying the early visual stages of reading. The goal of the initial stages of reading is to build up a representation of letter strings that is invariant for irrelevant perceptual dimensions, such as the location in the visual field, the color of the ink, the size and type of characters, and so forth. This abstract representation has been termed the “visual word form” (VWF) by Warrington and Shallice (1980). In normal subjects, words flashed within a single hemifield, either left or right of fixation, cause both hemifield-dependent occipital activations in contralateral retinotopic areas, and hemifield-independent activations in the left fusiform gyrus and other lateral temporal, parietal, and frontal areas of the left hemisphere (Cohen et al., 2000; Fiez & Petersen, 1998; Price, 1997). Within this extensive network, converging evidence suggests that a subregion of the left fusiform gyrus, whose Talairach coordinates are approximately $x = -43$, $y = -54$, $z = -12$, contributes crucially to the cerebral basis of the VWF (Cohen et al., 2000; Beauregard et al., 1997; Puce, Allison, Asgari, Gore, & McCarthy, 1996). It is activated irrespective of the stimulated hemifield, thus achieving invariance for position (Cohen et al., 2000). A study using masked repetition priming indicates that the VWFA responds to specific words independently of the case in which they are presented (Dehaene et al., 2001). Finally, this area seems to overlap with the critical lesion site for pure alexia, a selective deficit of word reading with sparing of writing and of auditory word comprehension (Leff et al., 2001; Beversdorf, Ratcliffe, Rhodes, & Reeves, 1997; Binder & Mohr, 1992; Damasio & Damasio, 1983; Dejerine, 1892). As a consequence of such converging evidence, we proposed to name this left fusiform region the visual word form area (VWFA) (Cohen et al., 2000).

The VWFA is thought to achieve positional invariance in letter string identification by receiving connections from both ipsi- and contralateral retinotopic areas (Figure 1). Neuropsychologists have long postulated that damage to those connections can be responsible for reading deficits (Binder & Mohr, 1992; Dejerine, 1892).

In particular, patients with lesions affecting the splenium of their corpus callosum are unable to read words presented in the left half of their visual field, a deficit that is thought to reflect an impaired transfer of visual information from low-level right-hemispheric visual regions to left-hemispheric regions specialized in written language processing (Cohen et al., 2000; Suzuki et al., 1998).

We used functional and diffusion tensor MRI to study the anatomical connectivity and reading circuitry in patient AC, a 26-year-old right-handed man. Surgery for a hemorrhage in his left mesial parietal lobe, due to a small arteriovenous malformation, left patient AC with a split of the posterior half of his corpus callosum (Figure 1) (Cohen et al., 2000; Intriligator, Henaff, & Michel, 2000; Michel, Hénaff, & Intriligator, 1996). At the time of testing, AC could read words normally when presented in his right hemifield, but was severely slowed and occasionally failed whenever words were presented in his left hemifield (Cohen et al., 2000; Michel et al., 1996) (see Methods for further details). The pattern of reading errors in patient AC can be explained by his callosal lesion, which created a disconnection between the right-hemispheric retinotopic areas and the left-hemispheric VWFA (Figure 1). In order to study the precise anatomical basis of this disconnection hypothesis, we first used fMRI to identify the inferotemporal regions activated during reading words presented tachistoscopically in one or the other hemifield. We then collected whole-brain diffusion tensor images in both the patient and 11 normal subjects. A statistical voxel-by-voxel comparison of the anisotropy images of the patient compared to normals allowed us to localize the degenerated connections. We then went back to the diffusion images of a normal subject to infer the premorbid direction of fibers in this area, and showed that they correspond in part to a long-distance fiber tract connecting right-hemispheric visual regions to the VWFA.

RESULTS

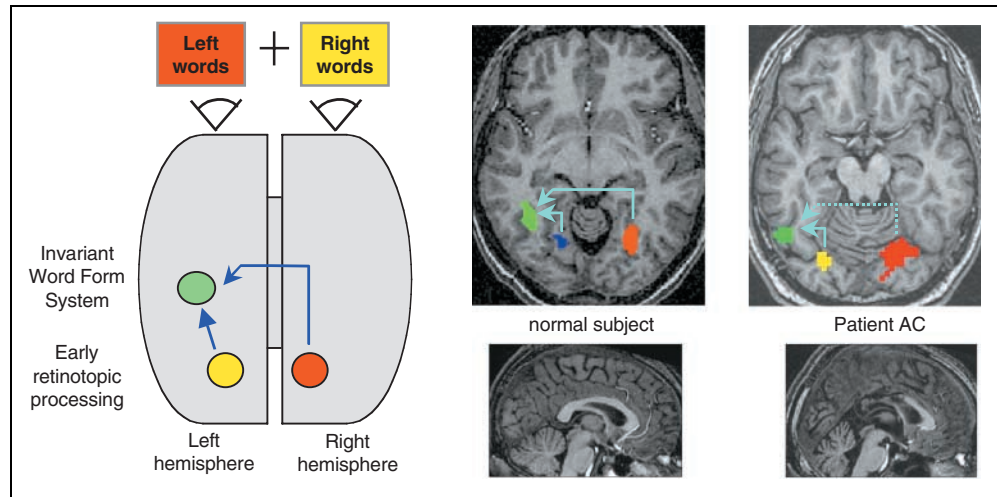
Behavior

Patient AC's reading behavior replicated earlier findings (Cohen et al., 2000; Michel et al., 1996). The patient experienced no difficulty in reading right visual field (RVF) words (2% errors, mean latency = 728 msec) and in saying the word “consonant” to RVF consonant string (0 errors, 1148 msec). However, he was significantly slower with LVF words than with RVF words, 2125 vs. 728 msec; $t(94 \text{ df}) = 7.67$, $p < 10^{-4}$, though his error rate remained almost at floor level (6% errors). There was no significant difference between hemifields for responses to consonant strings (1048 msec; 2% errors).

Functional MRI

To first identify the disconnected areas, fMRI images were collected in patient AC and in 9 control subjects

Figure 1. Left: schematic diagram of the brain architecture thought to support position-invariant identification of visual words. When a subject is engaged in reading words presented left or right of fixation, visual processing starts in contralateral retinotopic areas, which then project to a common left-hemispheric system, the visual word form, where an invariant representation of the letter string is constructed. In the case of words presented in the left hemifield, this implies an interhemispheric transfer of information across the corpus callosum. Middle: fMRI activations observed in a normal subject during reading of lateralized stimuli. The regions shown in red and yellow activated nonspecifically to alphabetic and checkerboard stimuli presented in the contralateral hemifield. The visual word form area, shown in green, activated to both left and right alphabetic stimuli. Right: fMRI activations observed in patient AC. The bilateral retinotopic activations were normal. Activation to alphabetic stimuli was present in the left fusiform gyrus at coordinates corresponding to the VWFA, but this region (shown in green) activated only when the stimuli were presented in the right hemifield. The sagittal T1 images at the bottom show the normal and lesioned corpus callosum.

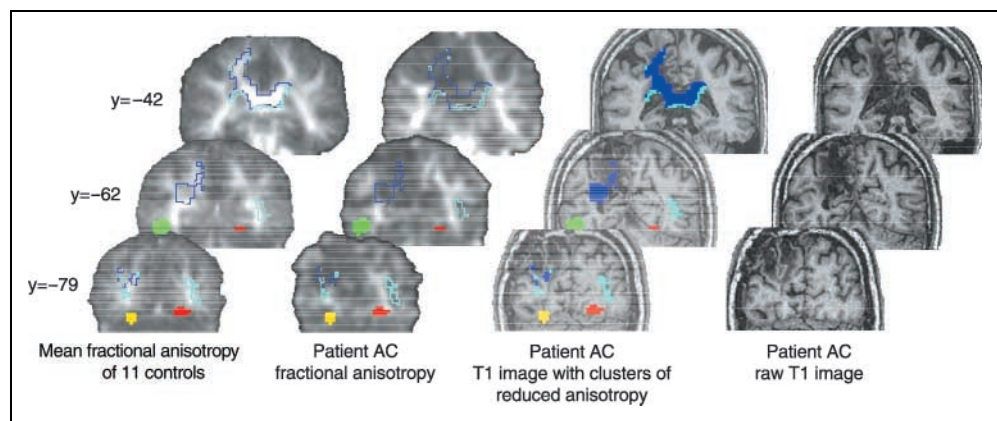


during passive presentation of high-frequency words, consonant strings, and checkerboards, in the left or right hemifield (total of 100 trials per condition) randomly intermixed in a fast-event related design (four series of 150 images; 1.5 T GE Signa scanner; TR = 2.4 sec, TE = 60 msec, FOV = 24 × 24 cm, resolution = 3.75 × 3.75 × 5 mm; 23 slices). In normals, a nonspecific retinotopic activation, showing greater activation to contralateral stimuli, whether they consisted of alphabetic strings or checkerboards ($p < .005$ each at the peak voxels), was observed in each hemisphere at coordinates close to those of area V4: left, TC 36 -72 -3, $t(8) = 20.5$;

right, TC -24 -81 -3, $t(8) = 7.07$; both $ps < 10^{-4}$. Those retinotopic activations were also present in patient AC: left, TC -24 -75 -18; $t(291) = 7.32$; right, TC 18 -75 -12, $t(291) = 8.64$; both $ps < 10^{-11}$.

In normals, a distinct left-lateralized and more anterior fusiform area showed a greater activation for alphabetic stimuli than for checkerboards, irrespective of whether they appeared in the left or in the right hemifield, $p < .005$ each at the peak voxel; TC -42 -57 -15; $t(8) = 4.61$; $p < 10^{-3}$. This location corresponds to previously published coordinates of the VWF area (Cohen et al., 2000). These findings confirm that this area

Figure 2. Localization of the regions with reduced fractional anisotropy in patient AC compared to 11 controls. Formal statistical comparison of anisotropy values in patient AC and in the 11 controls identified two regions with significantly reduced anisotropy. Within those regions, light blue is used to indicate voxels of reduced anisotropy where patient AC's T1 image was statistically indistinguishable from that of 40 normal subjects (hence presumably reflecting secondary degeneration distant from the original lesion). Dark blue indicates voxels of reduced anisotropy belonging to the lesion itself. In the leftmost column, those regions have been superimposed on images of mean anisotropy of 11 controls. In the second and third columns, their outline is shown superimposed on anisotropy images and T1 images from the patient. The rightmost column shows the raw T1 image for reference. For direct comparison with fMRI results, patient AC's fMRI activation clusters are shown as in Figure 1 (red = retinotopic activation to LVF stimuli; yellow = retinotopic activation to RVF stimuli; green = VWFA). It can be seen that the regions with reduced anisotropy form an almost continuous path whose endpoints stop close to the left and right hemisphere activations.



codes letter strings in a spatially invariant manner. In patient AC, a similar anatomical region was also activated more strongly by alphabetic stimuli than by checkerboards, but only when those stimuli appeared in the right hemifield, $TC = -45 -60 -12$; $t(291) = 6.50$; $p < 10^{-9}$.¹ When alphabetic strings were contrasted to checkerboards in the left hemifield, this region failed to activate at the conventional statistical threshold. Note, however, that a weakly significant effect was measured at the peak voxel of the patient's VWF area, $t(291) = 2.25$, $p < .05$. This difference between the patient and the controls was significant in a random-effect analysis of the difference in VWF activity induced by right-hemifield versus left-hemifield alphabetic stimuli, relative to checkerboards, $t(8) = 3.34$, $p < .01$ at the patient's peak voxel. The abnormal weakness of the activation of the patient's VWF by LVF alphabetic stimuli was also apparent when comparing it to the activation induced by RVF stimuli. In normals, the peak activation was not stronger for RVF than for LVF stimuli, $t(8) = 1.92$, $p < .1$, while this difference was highly significant in patient AC, $t(291) = 6.86$, $p < 10^{-9}$. Again this difference between the patient and the controls was significant in a random-effect analysis, $t(8) = 4.00$, $p = .004$ at the patient's peak voxel. We suggest that this abnormal deficit of activation of the left VWF area by left-hemifield words underlies patient AC's inability to read those words normally (Cohen et al., 2000).

Analysis of Diffusion Anisotropy

To demonstrate anatomically the disconnection of the left VWF area from contralateral visual regions, we

collected whole-brain diffusion tensor images in patient AC and in 11 normal controls (TR = 2.5 sec; TE = 82.4 msec, four repetitions of five regularly spaced b values in each of six directions, FOV = 24×24 cm, resolution = $128 \times 128 \times 2.8$ mm, 48 slices). To identify degeneration of white matter tracts in patient AC, images of fractional anisotropy (Pierpaoli & Basser, 1996) were compared voxel by voxel between the patient and the controls. The results revealed a significant drop of anisotropy in several sectors of the posterior left and right hemispheres (Figure 2). We studied the overlap of these regions with the lesion itself, defined formally by a statistical comparison of the patient's T1-weighted image with T1 images from 40 normal subjects ($p < .01$). This allowed us to distinguish two different clusters with reduced anisotropy (Table 1). A large set of voxels, which consistently corresponded to fiber bundles in normal subjects, were directly damaged by the lesion or were displaced by lateral ventricle enlargement in patient AC. However, decreased anisotropy was also observed in a second set of voxels outside of the lesion and distant from it. Those voxels were interpreted as indicating degeneration of white matter bundles. Indeed, they formed an almost contiguous set that spanned from the left ventral occipito-temporal region to its right homolog across the lesioned area of corpus callosum, in each case stopping a few millimeters from the areas found active in fMRI.

Diffusion Tensor Direction

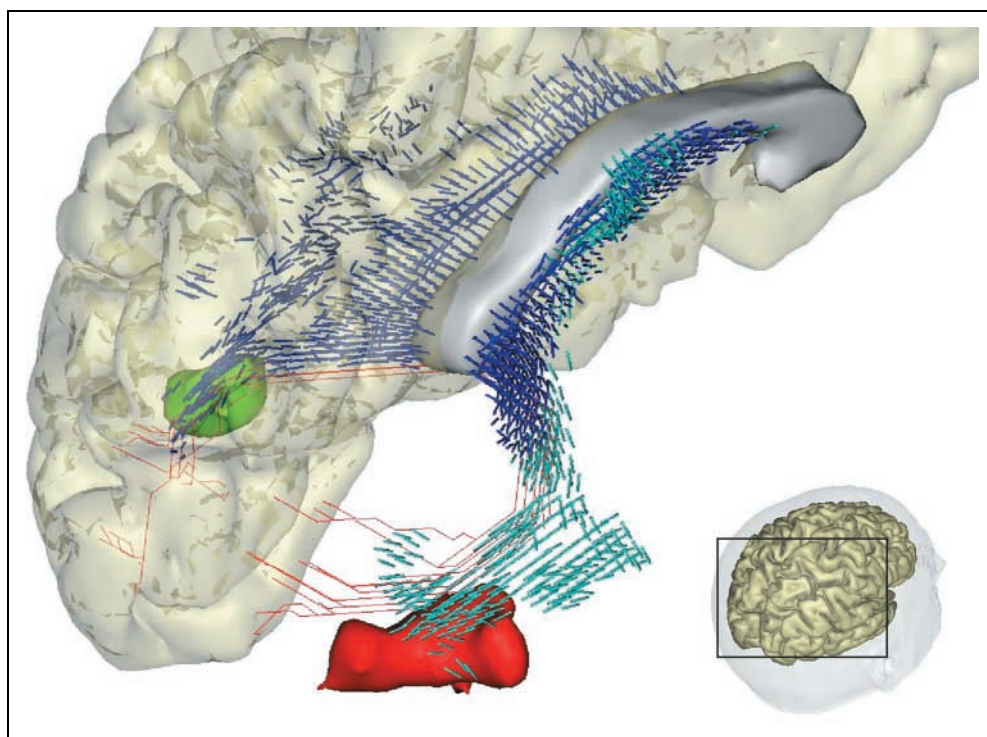
To reveal the topology of the impaired connections, we plotted in a normal subject, for each of the impaired

Table 1. Brain Regions Where Fractional Anisotropy Was Significantly Reduced in Patient AC Compared to 11 Normal Controls

<i>Anatomical Location</i>	<i>Talairach Coordinates of Local Maxima</i>	<i>Patient AC's Fractional Anisotropy</i>	<i>Normal Fractional Anisotropy (mean \pm 1 SD)</i>	<i>t Test</i>	<i>p Value</i>
Cluster 1: white matter underneath the right parieto-occipital junction, the fusiform gyrus and the middle occipital gyrus (89 voxels)	39, -57, 6	0.312	0.568 \pm 0.027	9.24	3E-06
	30, -78, 15	0.184	0.442 \pm 0.042	5.95	1E-04
	30, -81, 0	0.206	0.462 \pm 0.042	5.93	1E-04
Cluster 2: splenium, posterior half of callosum, bilateral major forceps, left mesial parietal lobe (1465 voxels)	0, -36, 15	0.177	0.758 \pm 0.032	17.46	8E-09
	-18, -36, 51	0.228	0.513 \pm 0.023	12.07	3E-07
	-18, -54, 36	0.193	0.517 \pm 0.035	8.80	5E-06
	-30, -69, 18	0.195	0.495 \pm 0.046	6.20	1E-04
	-30, -75, 15	0.208	0.450 \pm 0.049	4.42	1E-03
	12, -3, 30	0.271	0.641 \pm 0.032	10.88	7E-07
	-6, -9, 30	0.217	0.657 \pm 0.034	12.44	2E-07

Cluster 1 is located in normal-appearing tissue as seen on T1 images and is consistent with secondary degeneration of white matter tracts whereas Cluster 2, located in abnormal T1 region, is related to tissue directly damaged by the lesion.

Figure 3. 3-D representation of the postulated transcallosal fiber tract. This figure illustrates the tight match between the voxels with reduced anisotropy in patient AC (shown in blue) and the trackings obtained by computerized tracking of diffusion data from a normal subject (shown in red lines). The same color code as in Figure 2 is used (red cluster = patient AC's retinotopic fMRI activation to LVF stimuli; green = patient AC's VWFA; light blue = voxels with reduced anisotropy outside the T1 lesion; dark blue = voxels with reduced anisotropy inside the T1 lesion). Each blue vector represents the principal direction of the diffusion tensor in a normal subject, in voxels where patient AC showed significant reduced anisotropy. This representation suggests that the voxels with reduced anisotropy reflect the degeneracy of a transcallosal tract, which normally starts in the close vicinity of the right occipital cortex, passes over the posterior horns of the lateral ventricles and then through the splenium of the corpus callosum to the left occipito-temporal region.



voxels, the first eigenvector of the diffusion tensor, which indicates the principal direction of diffusion and therefore the main direction of neural fibers (Figure 3). The vectors aligned smoothly to form a bilateral tract, which started posteriorly in the white matter above the left and right fusiform gyri, passed over the posterior horns of the lateral ventricles, and joined in the splenium of the corpus callosum.

To confirm that the voxels with decreased anisotropy may correspond in part to a long-distance fiber tract connecting right-hemispheric visual regions to the VWFA, we used a fiber-tracking algorithm (Poupon et al., 2000). Within the large set of vector directions observed in the whole normal brain, this algorithm attempts to find chains of contiguous voxels along which the vector direction changes smoothly and which may, therefore, correspond to the trajectory of a main fiber tract. When the algorithm was seeded to trace long-distance connections in a normal brain starting from one of the voxels with anomalous anisotropy in patient AC, it often extracted transcallosal fibers joining the left and right occipito-temporal regions at various anteroposterior levels (Figure 3). Although the trajectory of those fibers was computed solely based on diffusion data from a normal brain, it closely matched the shape of the

region with decreased anisotropy in patient AC. This strengthens the hypothesis that the decreased anisotropy in patient AC reflects in part the degeneracy of an entire transcallosal fiber tract.

DISCUSSION

The combination of structural imaging techniques such as diffusion tensor imaging and functional imaging represent a promising approach for the study of brain connectivity and the analysis of disconnection syndromes. Combining both techniques in a posterior split brain patient, we showed that his left hemialexia could be related, functionally, to abnormal fMRI activations, and anatomically, to an impairment of connections between those activations. Using diffusion tensor imaging, statistical analysis revealed microstructural abnormalities at distance from the callosal lesions in regions without any T1-weighted MR signal changes and particularly in the white matter underlying right occipital cortical areas activated during reading. These microstructural alterations strongly suggest retrograde degeneration of a fiber tract crossing the lesioned area of the corpus callosum and running over the occipital horn of the lateral ventricle connecting the left ventral

occipito-temporal region to its right homolog. At the relatively coarse resolution used here (~ 3 mm), connections could not be traced to their precise final cortical targets, because diffusion tensor information became imprecise in the white matter just underlying the cortex, presumably due to the crossing of multiple fiber tracts. Furthermore, we do not claim that only the connections involved in position-invariant word identification were impaired. Rather, the lesion disconnected an extended set of bilateral ventral occipito-temporal areas. This agrees with previous behavioral evidence for impaired interhemispheric transfer of visual word, but also color and face information in patient AC (Intriligator et al., 2000).

Our study suggests that the left fusiform gyrus plays a crucial role in word reading by collecting and representing VWF information independently of its retinal location. Dejerine's (1892) initial interpretation of pure alexia was that the fusiform lesion severed two bundles of white matter, respectively, conveying visual information from the right- to the left-hemispheric primary visual cortex through the corpus callosum, and from left-hemispheric visual regions towards the left angular gyrus where word forms were thought to be stored. More recent studies allow us to update this initial anatomo-functional model. We now know that pure alexia can result from purely cortical lesions affecting the portion of the fusiform gyrus where the VWFA is found, but sparing the underlying long-distance connections (Beverdors et al., 1997). While such cases are not amenable to a disconnection account, other variants of pure alexia are still best explained by considering the connections of the VWFA originating from more peripheral visual regions, or heading towards lateral language cortex. The so-called subangular alexia that results from subcortical parietal lesions, presumably depriving the left inferior parietal lobule of its input, is thought to correspond to the latter mechanism (Iragui & Kritchevsky, 1991; Greenblatt, 1973). As for impairments of the input routes to the VWF area, the best documented situation corresponds to callosal lesions with a resulting alexia restricted to the left visual hemifield, as in the present case (Cohen et al., 2000; Suzuki et al., 1998). Suzuki et al. (1998) suggested that the critical portion of the callosum for the transfer of alphabetical information is the inferoposterior part of the splenium. From the study of lesion topography and reading abilities in several alexic patients, Binder & Mohr (1992) further proposed a schematic diagram of posterior callosal projections, suggesting that they run posterolaterally over the occipital horn of the lateral ventricle before reaching extrastriate visual cortex on the lateral and ventrolateral convexity. Our data are in good agreement with those neuropsychological inferences, and further reveal that the entire course of those fibers can now be traced in the normal human brain.

Contrary to Dejerine's initial hypothesis, the VWFA probably does not receive its main input from primary visual cortex. Rather, our fMRI results suggest that the stage of processing immediately prior to the VWFA is a retinotopic visual processing stage putatively identified as area V4, and present in both hemispheres (see Cohen et al., 2000). This predicts that it should be possible to observe a reading impairment symmetrical to callosal alexia, with pure alexia restricted to the right hemifield due to a disconnection depriving the VWFA of its visual inputs within the left hemisphere (see Figure 1). Indeed, such right hemialexia has been reported following a predominantly subcortical left occipito-temporal lesion, presumably depriving the VWFA of its input from the ipsilateral area V4 (Castro-Caldas & Salgado, 1984). It would be interesting to use diffusion tensor imaging in such a patient to examine if this would indeed show the predicted degenerated posterior fiber tract within the left hemisphere.

Conclusion

The present approach, based on the "negative tracking" of degenerated bundles can be used to isolate a neural pathway within the otherwise complex and intermingled connections of the normal human brain. While we applied it to a large impairment of interhemispheric connections, further studies will be needed to demonstrate the feasibility of this approach to the study of smaller intrahemispheric connections. This *in vivo* approach may be useful, not only in focal acquired lesions, but also to clarify the possible contribution of disconnections to degenerative diseases (Rose et al., 2000) or to developmental disorders such as developmental dyslexia (Klingberg et al., 2000).

METHODS

All experiments were approved by the regional ethical committee for biomedical research, and subjects gave informed consent. All scans were acquired using an 1.5T Signa horizon Echospeed MRI system (General Electric Medical Systems, Milwaukee, WI). Statistical analysis was done with SPM99 software.

Case Description

Patient AC was a 26-year-old right-handed man, with no significant medical history until the age of 22. His cognitive development and educational achievements were normal. About 4 years before the present study was carried out, he suffered from a hemorrhage in his left mesial parietal lobe. This hemorrhage was due to a small arteriovenous malformation, which was then surgically removed. The cerebral sequelae, as revealed by anatomical MRI, consisted of a split of the posterior half of his corpus callosum, with a lesion extending into the

left hemisphere up to the white matter of the superior parietal lobule. The right hemisphere was completely spared. His visual field was normal, and he showed no spatial neglect. Initially, he made 30–80% errors when reading aloud words presented in his LVF, while he could read normally words presented in his RVF. His performance improved over the following months and years through the use of compensation strategies, such as “semantic browsing” and letter-by-letter reading (see Michel et al., 1996 for a detailed description). However, his reading latencies remained abnormally long with LVF stimuli (Cohen et al., 2000).

Anatomical MR Imaging

High-resolution anatomical images were acquired in the axial plane using a spoiled gradient-echo sequence (124 slices 1.2-mm thick, TR = 10.3 msec, TE = 2.1 msec, TI = 600 msec) and 24 × 24-cm field of view (resolution of 0.937 × 0.937 × 1.2 mm). Images were normalized to Talairach space using a linear transform and the template of the Montreal Neurological Institute (MNI). To isolate patient AC’s lesion, we computed a two-sample *t* test between patient AC’s and 40 controls’ T1 images, after smoothing with a Gaussian kernel with full width at half maximum (FWHM) = 5 mm. We used a voxelwise significance level of .01, corrected to $p < .05$ for cluster extent.

Functional Imaging

Functional images were acquired in patient AC and in nine normal subjects. In each of four sequences, 150 functional volumes sensitive to blood oxygen level dependent contrast were acquired with a T2-weighted gradient-echo, echo planar imaging sequence (TR = 2400 msec, $\alpha = 90^\circ$, TE = 60 msec) and 24 × 24-cm field of view (resolution of 3.75 × 3.75 × 5 mm; 23 slices). Words, consonant strings, and checkerboards were presented in random order in the left and right hemifields (total of 100 trials per condition; SOA = 2400 msec; display duration = 200 msec; display eccentricity 2° to 6°). Word stimuli consisted of 168 frequent and highly imageable nouns (mean \log_{10} frequency per million = 1.75), three to six letters and one to three syllables in length. Consonant strings were matched to the words in length.

Images were corrected for different slice acquisition times and for subject motion, normalized to MNI coordinates, and smoothed (FWHM 5 mm). For each subject, the generalized linear model was used to fit each voxel with a linear combination of functions derived by convolving a standard hemodynamic response function with the known time series of the six stimulus types. An equal number of time-derivative functions modeled possible variations in activation onset. Degrees of freedom were adjusted for high-pass filtering (period 120 sec) and low-

pass filtering by a Gaussian function with a 4-sec width. We report here the single-subject analysis of patient AC (voxelwise $p < .001$, corrected $p < .001$ for cluster extent), and the random-effect analysis of the group of normal subjects (voxelwise $p < .01$, corrected $p < .05$ for cluster extent).

Behavioral Control

As a behavioral control to the fMRI experiment, the patient was presented with 200 word and consonant string stimuli drawn randomly from the original set of 336 stimuli. He was asked to name each word, and to utter the word “consonant” whenever he thought he was presented with consonant strings. Naming latencies were measured using a voice key, and all responses were recorded for subsequent scoring of errors.

Diffusion Tensor Imaging

Diffusion-weighted images were acquired in patient AC and 11 aged-matched controls with echo-planar imaging in the axial plane covering the whole brain (48 slices, 2.8 mm thick; TE = 84.4 msec, TR 2.5 sec) and 24 × 24-cm field of view (resolution 128 × 128). For each slice location, a T2-weighted image with no diffusion sensitization, followed by five *b* values (incrementing linearly to a maximum value of 1000 s/mm²) was obtained in six directions. In order to improve the signal-to-noise ratio, this sequence was repeated four times, providing 124 images per slice location. Before performing the tensor estimation, an unwarping algorithm was applied to the diffusion-weighted data set to correct for distortion related to eddy currents induced by the large diffusion-sensitizing gradients (Poupon et al., 2000). Thereafter, the diffusion tensor was calculated on a pixel by pixel basis as described (Pierpaoli & Basser, 1996). Images of fractional anisotropy (FA) were normalized to MNI coordinates using the linear transform calculated on the anatomical images, and smoothed (FWHM 5 mm). A two-sample *t* test was used to compare FA between patient AC and the controls. We used a voxelwise significance level of .01, corrected to $p < .05$ for cluster extent.

Reprint requests should be sent to Stanislas Dehaene, Unité INSERM 334, Service Hospitalier Frédéric Joliot, CEA, 4 Place du Général Leclerc, 91401 Orsay cedex, France, or via e-mail: dehaene@shfj.cea.fr.

The data reported in this experiment have been deposited in the fMRI Data Center (<http://www.fmridc.org>). The accession number is 2-2001-11256.

Note

1. As noted by Cohen et al. (2000), there is a variability among normals in the exact location of the VWFA. Though it is always found in the vicinity of the left occipito-temporal sulcus,

the Talairach coordinates show a standard deviation of about 5 mm in each direction. Furthermore, the VWFA in patient AC tends to be higher than in most controls, perhaps revealing a slight displacement following brain atrophy. Because of this variability, the axial slices in Figure 1 were centered on the main activation peak of the VWFA.

REFERENCES

- Beauregard, M., Chertkow, H., Bub, D., Murtha, S., Dixon, R., & Evans, A. (1997). The neural substrate for concrete, abstract, and emotional word lexica: A positron emission tomography study. *Journal of Cognitive Neuroscience*, *9*, 441–461.
- Beversdorf, D. Q., Ratcliffe, N. R., Rhodes, C. H., & Reeves, A. G. (1997). Pure alexia: Clinical-pathologic evidence for a lateralized visual language association cortex. *Clinical Neuropathology*, *16*, 328–331.
- Binder, J. R., & Mohr, J. P. (1992). The topography of callosal reading pathways. A case-control analysis. *Brain*, *115*, 1807–1826.
- Castro-Caldas, A., & Salgado, V. (1984). Right hemifield alexia without hemianopia. *Archives of Neurology*, *41*, 84–7.
- Cohen, L., Dehaene, S., Naccache, L., Lehéricy, S., Dehaene-Lambertz, G., Hénaff, M. A., & Michel, F. (2000). The visual word form area: Spatial and temporal characterization of an initial stage of reading in normal subjects and posterior split-brain patients. *Brain*, *123*, 291–307.
- Conturo, T. E., Lori, N. F., Cull, T. S., Akbudak, E., Snyder, A. Z., Shimony, J. S., McKinstry, R. C., Burton, H., & Raichle, M. E. (1999). Tracking neuronal fiber pathways in the living human brain. *Proceedings of the National Academy of Sciences, U.S.A.*, *96*, 10422–10427.
- Damasio, A. R., & Damasio, H. (1983). Anatomical basis of pure alexia. *Neurology*, *33*, 1573–1583.
- Dehaene, S., Naccache, L., Cohen, L., Le Bihan, D., Mangin, J. F., Poline, J. B., & Riviere, D. (2001). Cerebral mechanisms of word masking and unconscious repetition priming. *Nature Neuroscience*, *4*, 752–758.
- Dejerine, J. (1892). Contribution à l'étude anatomo-pathologique et clinique des différentes variétés de cécité verbale. *Mémoires de la Société Biologie*, *4*, 61–90.
- Fiez, J. A., & Petersen, S. E. (1998). Neuroimaging studies of word reading. *Proceedings of the National Academy of Sciences, U.S.A.*, *95*, 914–921.
- Geschwind, N. (1965). Disconnection syndromes in animals and man. *Brain*, *88*, 237–294.
- Greenblatt, S. H. (1973). Alexia without agraphia or hemianopsia. Anatomical analysis of an autopsied case. *Brain*, *96*, 307–316.
- Intriligator, J., Henaff, M. A., & Michel, F. (2000). Able to name, unable to compare: the visual abilities of a posterior split-brain patient [In Process Citation]. *NeuroReport*, *11*, 2639–2642.
- Iragui, V. J., & Kritchewsky, M. (1991). Alexia without agraphia or hemianopia in parietal infarction. *Journal of Neurology, Neurosurgery and Psychiatry*, *54*, 841–842.
- Klingberg, T., Hedehus, M., Temple, E., Salz, T., Gabrieli, J. D., Moseley, M. E., & Poldrack, R. A. (2000). Microstructure of temporo-parietal white matter as a basis for reading ability: evidence from diffusion tensor magnetic resonance imaging [see comments]. *Neuron*, *25*, 493–500.
- Le Bihan, D. (Ed.) (1995). *Diffusion and perfusion MR imaging: Application to functional MRI*. New York: Raven Press.
- Leff, A. P., Crewes, H., Plant, G. T., Scott, S. K., Kennard, C., & Wise, R. J. (2001). The functional anatomy of single-word reading in patients with hemianopic and pure alexia. *Brain*, *124*, 510–521.
- Michel, F., Hénaff, M.-A., & Intriligator, J. (1996). Two different readers in the same brain after a posterior callosal lesion. *NeuroReport*, *7*, 786–788.
- Pierpaoli, C., & Basser, P. J. (1996). Toward a quantitative assessment of diffusion anisotropy. *Magnetic Resonance in Medicine*, *36*, 893–906.
- Poupon, C., Clark, C. A., Frouin, V., Regis, J., Bloch, I., Le Bihan, D., & Mangin, J. (2000). Regularization of diffusion-based direction maps for the tracking of brain white matter fascicles. *Neuroimage*, *12*, 184–195.
- Price, C. J. (1997). Functional anatomy of reading. In R. S. J. Frackowiak, K. J. Friston, C. D. Frith, R. J. Dolan, & J. C. Mazziotta (Eds.), *Human brain function* (pp. 301–328). San Diego, CA: Academic Press.
- Puce, A., Allison, T., Asgari, M., Gore, J. C., & McCarthy, G. (1996). Differential sensitivity of human visual cortex to faces, letterstrings, and textures: A functional magnetic resonance imaging study. *Journal of Neuroscience*, *16*, 5205–5215.
- Rose, S. E., Chen, F., Chalk, J. B., Zelaya, F. O., Strugnell, W. E., Benson, M., Semple, J., & Doddrell, D. M. (2000). Loss of connectivity in Alzheimer's disease: An evaluation of white matter tract integrity with colour coded MR diffusion tensor imaging. *Journal of Neurology, Neurosurgery and Psychiatry*, *69*, 528–530.
- Suzuki, K., Yamadori, A., Endo, K., Fujii, T., Ezura, M., & Takahashi, A. (1998). Dissociation of letter and picture naming resulting from callosal disconnection. *Neurology*, *51*, 1390–1394.
- Warrington, E. K., & Shallice, T. (1980). Word-form dyslexia. *Brain*, *103*, 99–112.
- Werring, D. J., Toosy, A. T., Clark, C. A., Parker, G. J., Barker, G. J., Miller, D. H., & Thompson, A. J. (2000). Diffusion tensor imaging can detect and quantify corticospinal tract degeneration after stroke. *Journal of Neurology, Neurosurgery and Psychiatry*, *69*, 269–272.